Fluorescence Light Microscopy of Pulmonary Surfactant at the Air-Water Interface of an Air Bubble of Adjustable Size

D. Knebel,*† M. Sieber,* R. Reichelt,† H.-J. Galla,* and M. Amrein†

*Institut für Biochemie, Westfälische Wilhelms-Universität, D-48149 Münster, Germany; and †Institut für Medizinische Physik und Biophysik, Westfälische Wilhelms-Universität, D-48149 Münster, Germany

ABSTRACT The structural dynamics of pulmonary surfactant was studied by epifluorescence light microscopy at the air-water interface of a bubble as a model close to nature for an alveolus. Small unilamellar vesicles of dipalmitoylphosphatidylcholine, dipalmitoylphosphatidylglycerol, a small amount of a fluorescent dipalmitoylphosphatidylcholine-analog, and surfactant-associated protein C were injected into the buffer solution. They aggregated to large clusters in the presence of Ca^{2+} and adsorbed from these units to the interface. This gave rise to an interfacial film that eventually became fully condensed with dark, polygonal domains in a fluorescent matrix. When now the bubble size was increased or decreased, respectively, the film expanded or contracted. Upon expansion of the bubble, the dark areas became larger to the debit of the bright matrix and reversed upon contraction. We were able to observe single domains during the whole process. The film remained condensed, even when the interface was increased to twice its original size. From comparison with scanning force microscopy directly at the air-water interface, the fluorescent areas proved to be lipid bilayers associated with the (dark) monolayer. In the lung, such multilayer phase acts as a reservoir that guarantees a full molecular coverage of the alveolar interface during the breathing cycle and provides mechanical stability to the film.

INTRODUCTION

The surface tension of the highly solvated air-alveolar interface is strongly decreased by a molecular film of pulmonary surfactant (PS) at the air-saline interface. This function is needed to reduce the work of breathing and to provide stability to the alveoli of different size. PS is secreted by the alveolar type II epithelial cells (Bangham et al., 1979; Brown, 1964; Notter et al., 1980) and adsorbs to the interface. Neutral phosphatidylcholines represent 80% of its mass, one-half of it being the disaturated dipalmitoylphosphatidylcholine (DPPC). Five to 10% are the negatively charged phosphatidylglycerols (Shelly et al., 1982). From the four presently known surfactant-associated proteins named consecutively SP-A, -B, -C, and -D, the SP-C and SP-B play a decisive role with respect to the surface activity of the pulmonary surfactant. They are highly hydrophobic and co-purify with the lipids of the surfactant upon extraction of lung lavage with organic solvents (e.g., Hawgood, 1989; Johansson et al., 1994a; Possmayer, 1988; Shelly et al., 1982; Weaver, 1988).

Films of PS are distinct by a number of properties not found with pure films of any of its constituents alone. On the one hand, a monomolecular layer of the most abundant molecular species, DPPC, can reduce the surface tension close to zero, like the entire surfactant. Upon compression, the lipid molecules become aligned at the interface with the highly polar head-groups immersed in the aqueous phase and the hydrophobic tails directed to the air, until the film becomes incompressible. On the other hand, a pure DPPC-film does not keep the surface tension sufficiently low, when the interface is expanded as much as the alveolar interface becomes expanded during inhalation. The spacing between the molecules becomes too large for them to build up a sufficient film pressure. Pure DPPC-films are also susceptible to mechanical disturbance and collapse irreversibly when compressed beyond the point of minimum surface tension (Schurch et al., 1998). None of the other surfactant components does even allow, obtaining a very low surface tension in a pure film, because the molecules dissolve in the aqueous phase or the film collapses before a sufficient film pressure has built up. It is the hydrophobic proteins together with the lipids, necessary for a sustained reduction of the surface tension. DPPC, PG (or phosphatidylinositol), and either one of the two hydrophobic proteins, SP-C or SP-B, respectively, apparently represent a minimal functional system.

In this paper, we focus on the well-characterized functional system of SP-C, DPPC, and DPPG. SP-C is a small polypeptide with a molecular mass of 4 kDa. The carboxy terminal two-thirds of 33 to 35 amino acid residues (depending on the species), mainly valine and leucine, are ordered in a highly hydrophobic α-helix (Johansson et al., 1994b). The flexibly disordered amino terminal head group includes two palmitoylcysteinyls (Curstedt et al., 1990) and a positively charged arginine and lysine (Qanbar and Possmayer, 1995).

The structures of the film and like films have been studied extensively by fluorescence light microscopy

Submitted January 10, 2002, and accepted for publication February 28, 2002.

D. Knebel's present address is JPK Instruments AG, Bouchéstrasse 12, D-12435 Berlin, Germany.

Address reprint requests to M. Amrein, Institut für Hygiene und Arbeitsmedizin, Universitätsklinikum Essen, Hufelandstrasse 55, D-45147 Essen, Germany. Tel.: 49-0201-723-4591; Fax: 49-0201-723-5911; E-mail: matthias.amrein@gmx.de.

0006-3495/02/07/547/09 $2.00

(FLM), scanning force microscopy, mass spectrometry, and near field optical microscopy of films that were solvent-spread to the air-water interface of a Langmuir-trough and thereafter transferred onto a solid support at different states of compression (Amrein et al., 1997; Bourdos et al., 2000; Ding et al., 2001; Grunder et al., 1999; Kramer et al., 2000; Lee et al., 1997, 1998; Nag et al., 1996, 1999; von Nahmen et al., 1997b; Perez-Gil et al., 1992). Moreover the film balance represents a planar lipid monolayer, whereas the alveolar monolayer is strongly curved.

Thus, in the present study, we carried-out FLM in a novel manner to reveal how the film organizes when matter becomes adsorbed to the interface from the aqueous phase and how the film rearranges when the interface is compressed thereafter. FLM is commonly performed by placing a microscope objective closely over some film at the interface of a Langmuir trough. However, this set-up is not well suited for the observation of structural dynamics, because some film area moves out of the field of view of the microscope as soon as the film is compressed or decompressed, respectively. Furthermore, mechanical vibrations and airflow frequently cause motion of the films. In the present study, an air bubble was used instead of a conventional film balance and the film viewed through an immersion-objective from the aqueous phase. Whereas bubbles have long been recognized as a means to evaluate surface activity of pulmonary surfactant (Enhorning 1977; Schurch et al., 1998), they were not used for the purpose of microscopy in situ.

MATERIALS AND METHODS

Engineering of air bubbles

Air bubbles of 50 to 500 μm in diameter were produced in a buffer solution. They were anchored to hydrophobic areas on an elsewhere-hydrophilic mica support. The hydrophobic areas (size: 100 $\times$ 100 μm, 8 patches per mm) were made by evaporating Cr (3 nm) and then Au (5 nm) onto freshly cleaved mica across a mask in a high vacuum apparatus. Then, the sample was soaked for 30 min in 1 mM octanthiol (Fluka, Neu-Ulm, Germany) and rinsed extensively in ethanol per analysis (Merck, Darmstadt, Germany) and Milli-Q-water (Milli-Q_{185}Plus, Millipore GmbH, Eschborn, Germany). This resulted in a hydrophobic, self-assembled monolayer of octanethiol, chemisorbed to the gold-covered areas, whereas the mica regions remained uncovered. Now, a drop of buffer containing 25 mM Hepes and 3 mM $CaCl_2$ (pH 7.0) was placed on the support. Subjecting the sample to reduced air pressure (20 kPa) in an airtight chamber resulted in the growth of bubbles adherent to the hydrophobic patches. The hydrophilic mica paths between the hydrophobic areas prevented the bubbles from spreading from hemispherical to a more flattened shape and kept the amphiphilic molecules from creeping from the air-water interface onto the support after an interfacial film had been adsorbed (see below). Once the bubbles had formed, the pressure was slowly increased to ambient and most of the buffer was replaced by fresh, air saturated solution to prevent the bubbles from dissolving again.

Film formation at the air-water interface

To obtain a molecular film of pulmonary surfactant at the air-water interface of the bubbles, small unilamellar vesicles were allowed to adsorb to the interface. We used a model surfactant system consisting of 1,2-dipalmitoyl-*sn*-glycero-3-phosphocholine (DPPC), 1,2-dipalmitoyl-*sn*-glycero-3-(phospho-rac-(1-glycerol)) (DPPG) (4:1 molar ratio), SP-C (0.4 mol%), and 2-(4,4-difluoro-5-methyl-4-bora-3a, 4a-diaza-*s*-indacene-3-dodecanoyl)-1-hexadecanoyl-*sn*-glycero-3-phosphocholin (BODIPY-PC) as a fluorescent DPPC-analog (0.4 mol%). Vesicles of this system were prepared as described in Woodle and Papahadjopoulos (1989). DPPC and DPPG were purchased from Avanti Polar Lipids Inc. (Alabaster, AL). BODIPY-PC was purchased from Molecular Probes Inc. (Eugene, OR). Recombinant dipalmitoylated surfactant-associated protein C (SP-C) was a generous gift from Byk-Gulden Pharmaceuticals (Konstanz, FRG) (Schilling et al., 1987)). The vesicles were added to the sample to a final phospholipid concentration of 0.02 mM.

FLM measurements

For conventional fluorescence microscopy (see Figs. 2–5 and 8) an STM5-MJS epifluorescence microscope (Olympus, Hamburg, Germany) was used with an immersion objective (60$\times$, NA 0.9). Film formation and compression was monitored by video films acquired by a Proxicam CCD-camera equipped with an image intensifier (Proxitronic, Bensheim, Germany).

For the confocal light microscope image (see Fig. 6), an immersion objective (63$\times$, NA 1.32) and a pinhole size of 2.5 optical units were used in a commercial microscope (TCS 4D Leica, Heidelberg, Germany), BODYPY-PC fluorescence was excited with the 488-nm line of an air-cooled Ar-Kr laser, and emission was measured beyond 510 nm. Data acquisition was performed with eightfold frame averaging. Under these experimental conditions, lateral and axial resolutions of 0.27 and 0.49 μm, respectively, are obtained (Kubitscheck and Peters, 1998). Care was taken to exploit the 8-bit dynamic range of the instrument fully. Laser power was adjusted such that no significant photobleaching occurred during the experiment.

Changing the bubble size

The pressure p_0 in the chamber (Fig. 1) containing the bubbles was decreased to p_{actual} to increase the interfacial area from A_0 to A_{actual} and vice versa. Given a spherical geometry and neglecting the (minor) pressure difference from within the bubble to the pressure in the chamber, the relative interfacial area x_A is

$$x_A = \frac{A_{\text{actual}}}{A_0} \approx \left(\frac{p_{\text{actual}}}{p_0}\right)^{-2/3}$$

Note that the maximal possible area in such system is obtained when the chamber pressure corresponds to the vapor pressure of water (2.34 kPa at 20°C for pure water).

RESULTS AND DISCUSSION

Vesicle adsorption

Small unilamellar vesicles were added to the Ca^{2+}-containg buffer to a final phospholipid concentration of 0.02 mM, and the aqueous phase was not stirred. This low concentration and the absence of stirring allowed observing the vesicle adsorption and the film formation over a period of several hours before an end-point was reached. On the other hand, stirring led to an immediate film formation (see below).

The vesicles aggregated to clusters of several micrometers in size even before a film at the interface had visibly

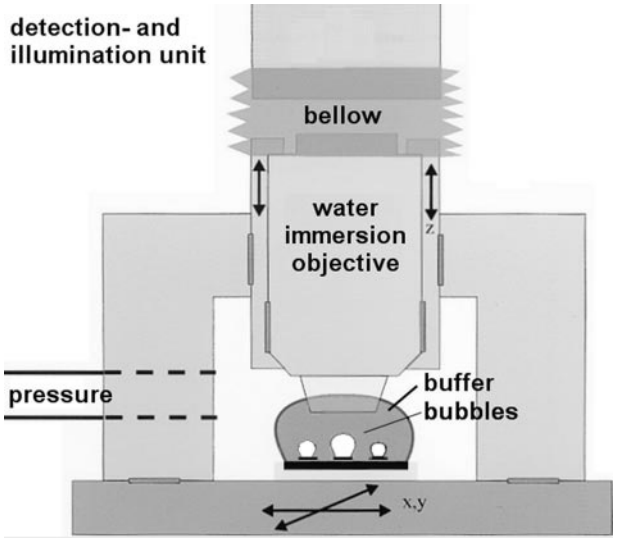

FIGURE 1 Experimental setup. The sample was contained in an airtight chamber. Air bubbles in the range of 50 to 500 μm in diameter were submersed in buffer. They were anchored to hydrophobic areas on an elsewhere-hydrophilic mica support. The interfacial film formed from vesicles, injected into the buffer. The film was viewed from above across the immersion light microscope objective. The objective was sealed into the chamber but could be moved up and down to focus. The chamber was mechanically detached from the illumination and detection unit.

formed. The clusters often adhered to the bubble surface (Fig. 2), giving rise to an open, sponge-like halo around the bubble.

When Ca^{2+} was absent in the buffer solution, there were no visible clusters present, and films did not form at the interface. This clearly shows the important role of Ca^{2+}, which is known to strongly reduce the repulsion between negatively charged surfaces in water and therefore allows the negatively charged vesicles to come close to each other and to some preformed film at the air-water interface and to get into physical contact (Israelachvili 1997). When Ca^{2+} was removed from the buffer, after the interfacial film had already been formed, the clusters in the aqueous phase disintegrated and the halo around the bubble disappeared. However, the film itself did not apparently change. Hence, vesicles merely in physical contact to each other formed the clusters. At the interface, however, a film had irreversibly formed.

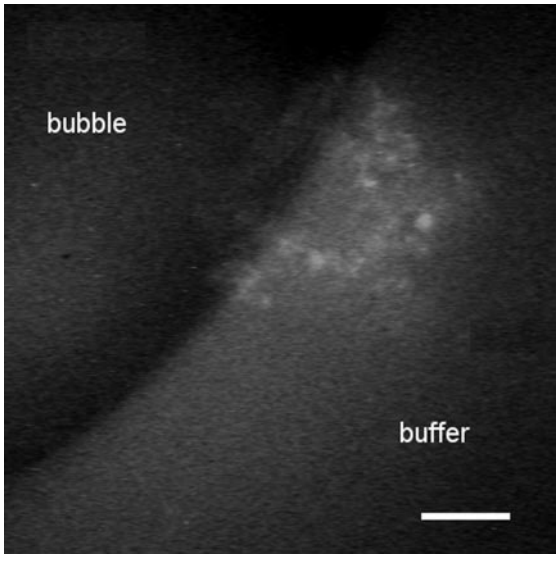

FIGURE 2 Optical section across an air bubble after vesicles were allowed to adsorb. In the presence of Ca^{2+}, the vesicles formed clusters. They adhered to the interface to form a halo around the bubble. The bar corresponds to 25 μm.

Film formation

In an early stage, the film at the air-water interface showed dark patches that diffused in a fluorescent matrix (Fig. 3). Apparently, the bright (dye-containing) area was in a fluid state, whereas the dark areas (devoid of the dye) were condensed. Note that in the case of films of a single lipid-species, two coexisting phases (liquid expanded and liquid condensed, respectively) are indicative of a phase transition of first order. In the case of the mixed film under investigation, the coexistence of two phases may be additionally attributed to the segregation of the different components with some component being condensed and some other component still being in a fluid state. We showed earlier that the fluid phase contains the SP-C in addition to the fluorescent dye and a fraction of the lipids (Bourdos et al., 2000; von Nahmen et al., 1997a). The dark, condensed phase consists of purely lipid.

The dark lipid patches apparently repelled each other when they came close. This may be attributed to an electrical surface potential within these areas causing the repulsion when the electrical fields of two approaching patches started to overlap. Both, DPPC as well as DPPG, posses a substantial electrical dipole moment in direction of the molecular axis that gives rise to the surface potential, once the molecules become aligned in a condensed phase (Möhwald, 1990; Oliveira and Bonardi, 1997). Note that the surface potential not only causes two patches to become repelled by each other but also determines the size and shape of these areas (Möhwald 1990).

Interestingly, many of the condensed patches harbored bright areas (denoted by arrows in Fig. 3 *A*). They were often brighter than the fluid phase, and in cases there were several distinct levels of brightness present. An earlier study by scanning force microscopy revealed that such bright areas within dark patches consist of at least one additional lipid bilayer on top of monomolecular areas of condensed lipid (Wintergalen 1999). Sometimes the bright matter extended into the buffer as one of the above-described clusters of vesicles that formed the halo around the bubble. This indicates that the adsorption of vesicles takes place in the

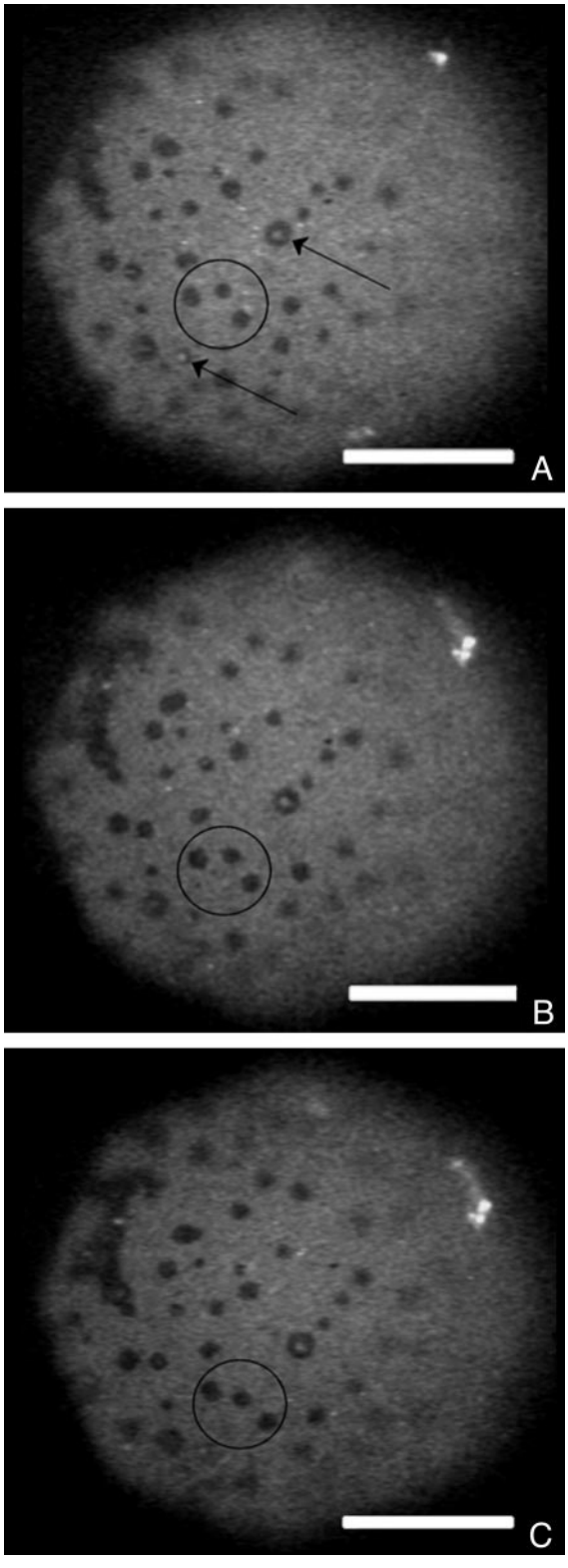

FIGURE 3 Three FLM micrographs from a video sequence of a film in an early stage of the film formation. The images shown are ~3 s apart from each other. The aqueous phase was not stirred to be able to observe the process. Condensed lipid rafts (*dark*) diffused in a fluid matrix that also contained the fluorescent dye. The rafts repelled each other when they came close and were never observed to merge. The circle denotes threerafts that changed very noticeably their relative position with time. The arrows denote rafts that contain a bright spot, more and more commonly observed with increasing adsorption time. The bright spots have been found to consist of additional lipid bilayers or aggregates of vesicles adherent exclusively to condensed rafts. The bar corresponds to 25 μm.

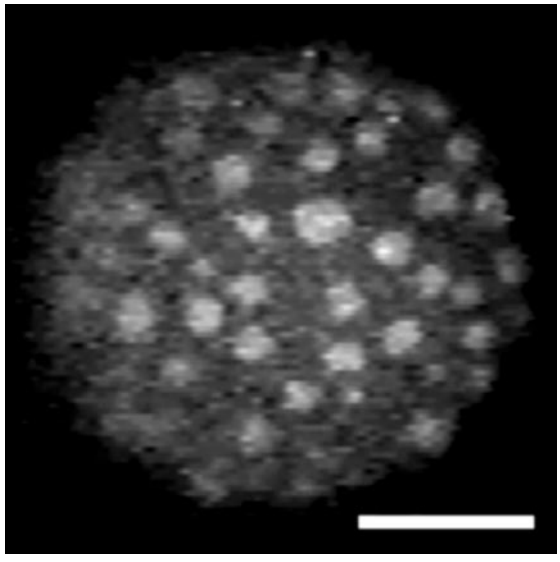

FIGURE 4 FLM micrograph from a video sequence of a film in an early stage of the film formation. Interestingly, here, bright rafts diffuse in a darker matrix. The rafts apparently consist of a condensed lipid monolayer that is fully covered by at least one additional bilayer. The bilayer contains the fluorescent DPPC-analog. The bright areas clearly show several distinct levels of brightness corresponding to distinct numbers of additional bilayers. The bar corresponds to 25 μm.

condensed phase. On some bubbles, the contrast even appeared reversed as compared with Fig. 3 (Fig. 4), and bright patches were diffusing within a darker matrix. In these cases, the condensed locations of the film were apparently fully covered by additional lipid bilayers. It is noteworthy that Figs. 3 and 4 were taken from the same sample immediately one after the other but from two different air bubbles.

With time, the interfacial film got at rest (Fig. 5 *A*). Fluorescent areas with distinct levels of brightness were dispersed within areas devoid of dye. The film structure did no longer change over a prolonged period of time (Fig. 5 *B*). However when the film was now disturbed mechanically, the structure became more regular with a bright mesh, surrounding dark polygonal areas (Fig. 5 *C*). Similar films could be obtained within a time scale of seconds to minutes, when the buffer was stirred during the adsorption (Fig. 6). It is therefore concluded that this structure represents the equilibrium state of the film. The model system under investigation is known to reach an equilibrium surface pressure of ~50 mN/m (Post et al., 1995), like the equilibrium

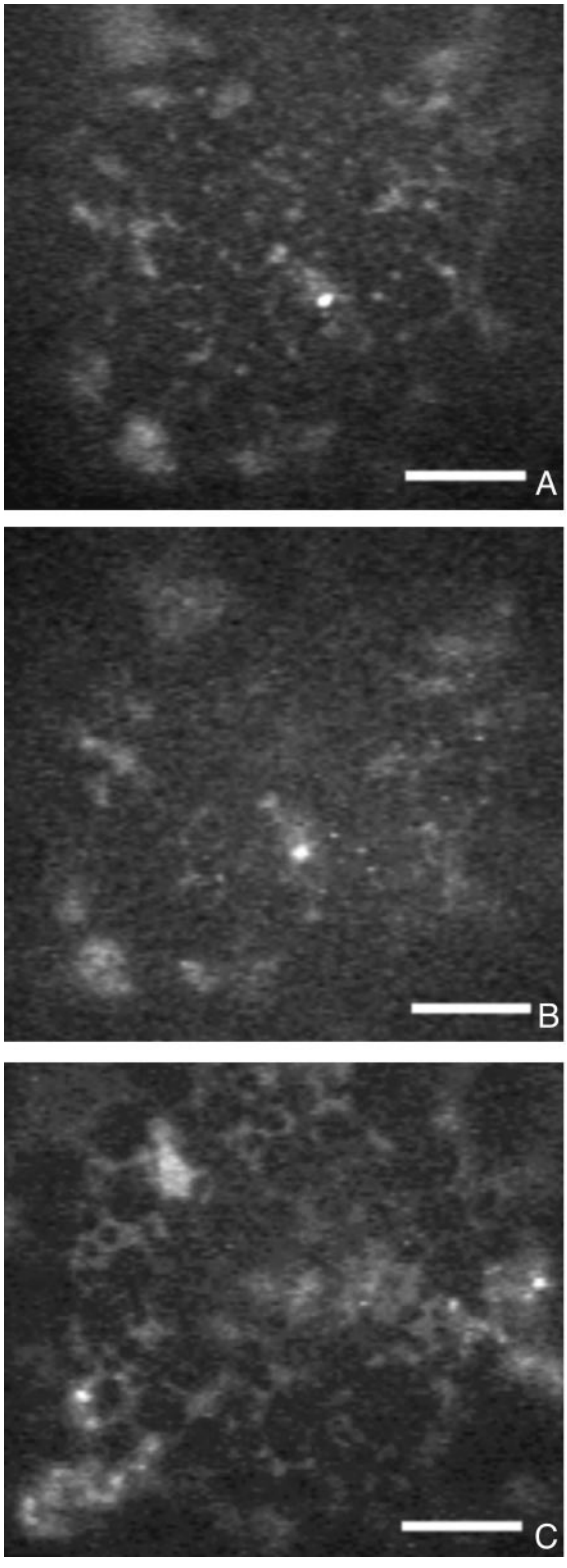

FIGURE 5 FLM micrographs of the interfacial film, after the adsorption had become complete. The aqueous phase was not stirred and the process of film formation had taken several hours. After that, the structure no longer changed and the film showed no more motion (*A* and *B* have been taken ~10 h apart). Under these conditions the final film showed no regular pattern. However, when the film was mechanically agitated, the structure rearranged. A fluorescent mesh surrounded areas that were devoid of fluorescent dye (*C*). A similar structure as in *C* was obtained within minutes or even seconds when the aqueous phase was stirred (see Fig. 6).

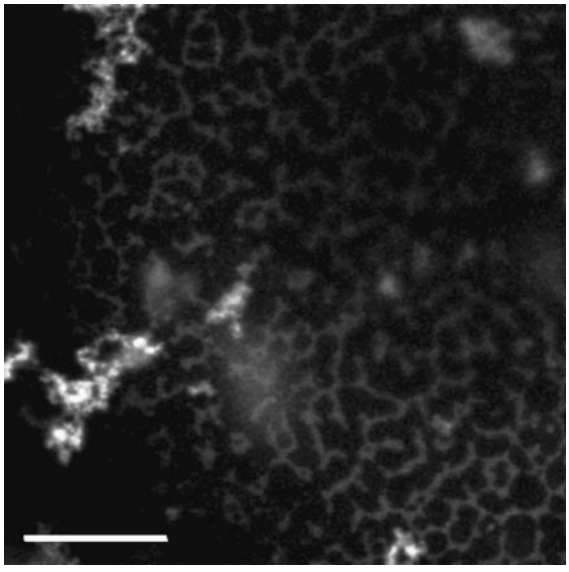

FIGURE 6 Three-dimensional dataset from a confocal-FLM of a bubble after the film formation had become complete. The aqueous phase was stirred and the interface was fully covered by the condensed film within a time scale of seconds to minutes. It is composed of a fluorescent mesh surrounding dark patches as in Fig. 5 *C*. In addition to the film, there are large clusters of vesicular matter that are tightly anchored to the bubble surface. Apparently, the film formed from these extended clusters. The dataset is composed of eight optical sections covering an overall focus depth of 5 μm. The bar corresponds to 25 μm. The apex of the bubble lies in the direction of the upper right corner outside the image.

surface pressure of surfactant extracted from animal lungs. Hence, the films of Figs. 5 and 6 are assumed to be in this condensed state.

A recent study by scanning force microscopy directly at the air-water interface revealed that the bright areas consisted of lipid bilayers, adherent to the interfacial film (Knebel et al., 2002). Interestingly, a similar film structure has also been observed with films that had been spread from an organic solvent to the interface of a Langmuir trough, compressed thereafter by the movable barrier, and transferred onto a solid support for FLM and scanning force microscopy (von Nahmen et al., 1997b): the matter formed stacks of lipid bilayers in the bright areas, as soon as the films were compressed beyond the point of their equilibrium surface pressure. This matter reinserted fully into the film upon expansion. Apparently, each SP-C molecule was associated with a defined number of lipid molecules (Kramer et al., 2000). Taken these earlier findings and the above-described results together, the film may have formed as follows (Fig. 7). 1) Large aggregates of the vesicular matter adsorbed to the interface rather than isolated vesicles.

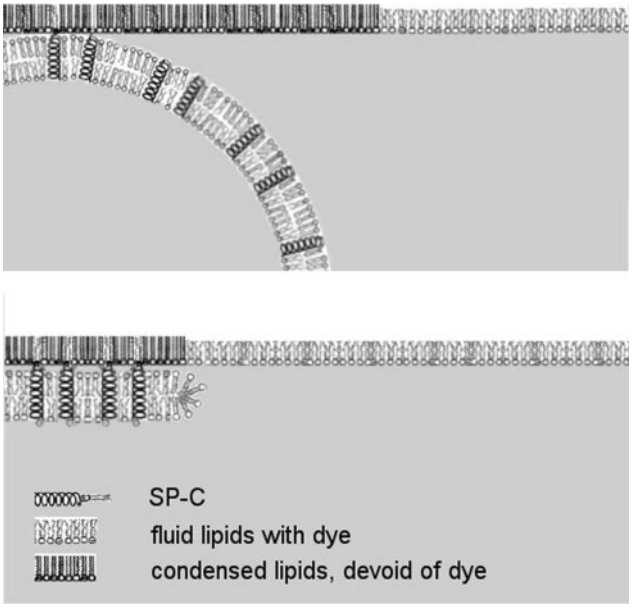

FIGURE 7 Vesicular matter apparently adsorbs exclusively to condensed locations of the interfacial film. It then either inserts itself into the film or forms single or multiple stacks of lipid bilayers.

2) The matter formed a monomolecular layer with rafts of condensed lipids, diffusing in a fluid matrix. 3) The rafts served as a template, where additional aggregates adhered. Some of the matter inserted into the monolayer and some reorganized into single and multiple lipid bilayers. 4) The film then rearranged into highly condensed areas of a purely lipid monolayer, surrounded by the above described multilayered regions that contained the SP-C. Even in the latter regions, the first monolayer in direct contact with the air-water interface may have consisted of highly condensed lipids.

A film formation from large aggregates may be important for the proper function of surfactant in the lung. New surfactant matter is delivered to the interface much faster in large clusters than would be through the diffusion-limited adsorption of small vesicles. This may be important when the air-water interface is formed for the first time after birth and when part of the surface-active film gets lost through inactivation. The current observation is in line with adsorption studies, performed by the captive- and the pulsating bubble surfactometer (Goerke and Clements, 1986; Schurch et al., 1994). The surface tension decreased in discrete steps (adsorption clicking) rather than continuously. The authors assessed the cooperative insertion of up to 10^{14} lipid molecules per single step.

The local formation of lipid bilayer structures and multiples thereof is a characteristic of the specific model surfactant system used here, but also of any other functional surfactant. It depends on the presence of either SP-C or SP-B or both. Similar structures have in fact been found with films containing SP-B instead of SP-C or animal lung extract, containing both proteins (Krol et al., 2000; Lipp et al., 1998).

The unique structural organization of the film is based on specific lipid-protein interactions. First, our current observations and earlier findings showed that bilayers are always found in association with condensed lipid areas and never with fluid lipid areas. This may result from a specific interaction of the two palmitoyl-groups of the SP-C with the monolayer. They may specifically insert themselves in the condensed areas of the monolayer as the first step of the adsorption of new matter from vesicles. Thereby they may act as a hydrophobic anchor that ensures a tight contact of the bilayers to the monolayer. This function has also been demonstrated by observing the film pressure of a purely lipid film on a film balance upon the adsorption of vesicles that also contained SP-C (Wintergalen 1999). When the vesicles were added to the subphase under conditions, where fusion of the vesicles with the monolayer was not taking place (i.e., in absence of calcium ions), the film pressure rose nevertheless. This increase in surface pressure was not observed, when the two palmitoyl-groups had been removed from SP-C beforehand. It is interesting to note that palmitoyl-groups also constitute the lipid-anchor of many of the proteins, associated with sphingolipid rafts in the outer leaflet of cell membranes. There, too, the association is specifically with the condensed, fully saturated lipids of the rafts (Simons and Toomre, 2000). This points to the general role of palmitoyl-groups to anchor proteins specifically to condensed regions of lipid layers.

Although the palmitoyl-groups of the SP-C are apparently associated with the condensed lipids of the first monolayer at the air-water interface, the helical part of the SP-C is known to span lipid bilayers in a fluid state but is excluded from bilayers in the condensed gel phase (Johansson and Curstedt, 1997). Hence, SP-C may cross-link the condensed monolayer of saturated lipids to fluid bilayers that can also contain unsaturated lipids. It is tempting to believe that in the lung, where unsaturated lipids make up a substantial amount of the surfactant lipids, SP-C also causes sorting, directing the unsaturated lipids to the bilayers and the saturated lipids to the monolayer. A full coverage of the monolayer with saturated lipids may in fact be prerequisite for the low surface tension of the interface observed in the lung.

Expansion and compression

After vesicle adsorption, the interfacial area of the bubble of Fig. 8 was increased by approximately one-third of its original size by reducing the environmental pressure from 100 kPa to ~65 kPa (Fig. 8 *A*). Before, all excessive vesicles had been removed by exchanging the subphase several times by a buffer devoid of Ca^{2+}. Notwithstanding the large expansion, the film remained in a condensed state as it was still fully at rest. The bubble was then decreased

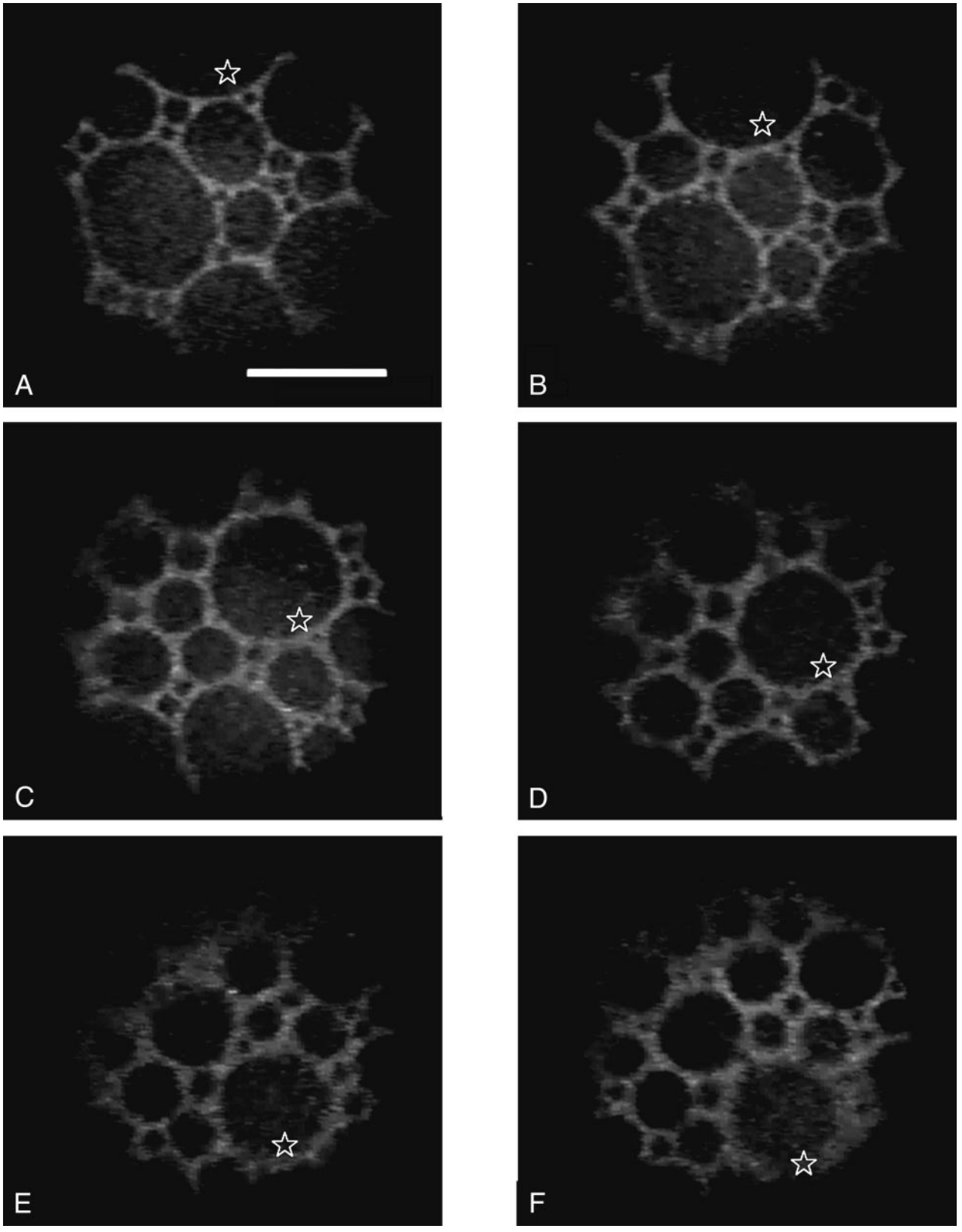

FIGURE 8 Six FLM micrographs from a video sequence of a compression cycle of an air bubble. The diameter of the bubble is decreased and, hence, the surface film compressed (from *a* (100%) to *f* (75%)). A fluorescent mesh becomes increasingly broader upon compression to the debit of the dark domains. This is indicative of the formation of more and more multilamellar structures in the bright areas that act as a surface-associated reservoir. Note that the area in view slightly moved in direction from the upper to the lower part of the image. The asterisk denotes a common point in the film. The bar corresponds to 25 μm.

incrementally to its original size (Fig. 8, *B–F*). It is noteworthy that the observed area of the film remained mostly in view of the microscope during the process of expansion and compression. This is unlike the situation of FLM on a Langmuir-trough, where some observed area always moves out of view of the microscope, as soon as the film is compressed or decompressed, respectively.

Upon compression, the fluorescent rims became broader and the dark areas smaller. Note that this behavior is apparently in contrast to what is commonly observed with liquid expanded films under compression. However, in the case of liquid expanded films, a bright, fluid monolayer phase becomes increasingly a condensed (dark) monolayer phase, whereas here, a condensed monolayer phase undergoes a transition into a (bright) multilamellar phase upon compression. In both cases, the process is reversible.

The expansion and compression cycles demonstrate the function of the SP-C to build up a surface-associated reservoir that guaranties a full molecular coverage of the interface, when the interface is increased. It mediates the motion of the lipids forth and back between the monolayer and the bilayer phase. The more the film becomes compressed, the more of the surfactant matter is "stored" in single as well as multiple lipid bilayers. The fluorescent areas exhibit several distinct levels of brightness, presumably reflecting the number of bilayers stacked on top of each other. Our results are consistent with surface-activity studies by the captive bubble technique of a comparable system (Schurch et al., 1998). After de novo formation of an interfacial film, Schürch and his associates found that the matter associated with the interface was sufficient to cover up to six times the original area, depending on the presence of SP-C (these films consisted of PG/DPPC and had a SP-C content of 1% w/w). Hydrophobic extracts of surfactant from natural sources had formed a reservoir of at least two additional monolayers after adsorption.

Conclusions and future perspectives

The current study strengthens and expands our earlier findings of an interfacial film, composed of multilamellar areas and monomolecular regions as the basic principal of a functional PS. The novel experimental approach chosen here, allowed directly observing the formation and function of the interfacial film, where as formerly, only a static picture of the film could be obtained.

The authors view the merits of the novel approach to be generally applicable to the study of the dynamic structure of molecular films at interfaces. 1) Contraction and expansion of the film occurs symmetrically to the optical axis of the microscope to the result that some film area remains in the field of view during this procedure. 2) The interface is fully protected from outside-disturbance. 3) Because of the small sample volume, very little of the surface-active substance under investigation is required.

The setup is currently upgraded by the simultaneous measurement of the surface tension of the interface. The shape of the bubble is a function of surface tension and may be used for this latter measurement (Andreas et al., 1938; Schurch et al., 1998; Skinner et al., 1989). This will then allow observing directly the structure-function relationship of pulmonary surfactant and any other surface-active substance.

We acknowledge L. Melanson for careful corrections, Dr. U. Kubitschek for his collaboration to obtain Fig. 6. This work was supported by the IMF (Innovative Medizinische Forschung) at the University of Münster, Germany (grant RE-1-5-II/96-16 and RE-1-5-II/97-26) and the DFG (grants SFB 424, Si 670, and AM III/3–1).

REFERENCES

Amrein, M., A. von Nahmen, and M. Sieber. 1997. A scanning force- and fluorescence light microscopy study of the structure and function of a model pulmonary surfactant. *Eur. Biophys. J.* 26:349–357.

Andreas, J. M., E. A. Hauser, and W. B. Tucker. 1938. Boundary tension by pendant drops. *J. Phys. Chem.* 42:1001–1019.

Bangham, A. D., C. J. Morley, and M. C. Phillips. 1979. The physical properties of an effective lung surfactant. *Biochim. Biophys. Acta.* 573: 552–556.

Bourdos, N., F. Kollmer, A. Benninghoven, M. Ross, M. Sieber, and H. J. Galla. 2000. Analysis of lung surfactant model systems with time-of-flight secondary ion mass spectrometry. *Biophys. J.* 79:357–369.

Brown, E. S. 1964. Isolation and assay of dipalmitoyl lecithin in lung extracts. *Am. J. Physiol.* 207:402–406.

Curstedt, T., J. Johansson, P. Persson, A. Eklund, B. Robertson, B. Löwenadler, and H. Jörnvall. 1990. Hydrophobic surfactant-associated polypeltides: SP-C is a lipopeptide with two palmitoylated cycteine residues, whereas SP-B lacks coralently linkes fatty acyl groups. *Proc. Natl. Acad. Sci. U.S.A.* 87:2985–2989.

Ding, J., D. Y. Takamoto, A. von Nahmen, M. M. Lipp, K. Y. Lee, A. J. Waring, and J. A. Zasadzinski. 2001. Effects of lung surfactant proteins, SP-B and SP-C, and palmitic acid on monolayer stability. *Biophys. J.* 80:2262–2272.

Enhorning, G. 1977. A pulsating bubble technique for evaluating pulmonary surfactant. *J. Appl. Physiol.* 43:198–203.

Goerke, J., and J. A. Clements. 1986. Alveolar surface tension and lung surfactant: handbook of physiology: the respiratory system: mechanics of breathing. Bethesta, MD. *Am. Physiol. Soc.* 3:247–261.

Grunder, R., P. Gehr, H. Bachofen, S. Schurch, and H. Siegenthaler. 1999. Structures of surfactant films: a scanning force microscopy study. *Eur. Respir. J.* 14:1290–1296.

Hawgood, S. 1989. Pulmonary surfactant apoproteins: a review of protein and genomic structure. *Am. J. Physiol.* 1:13–22.

Israelachvili, J. N. 1997. Intermolecular and Surface Forces. Academic Press, London. 296.

Johansson, J., and T. Curstedt. 1997. Molecular structures and interactions of pulmonary surfactant components. *Eur. J. Biochem.* 244:675–693.

Johansson, J., T. Curstedt, and B. Robertson. 1994a. The proteins of the surfactant system. *Eur. Respir. J.* 7:372–391.

Johansson, J., T. Szyperski, T. Curstedt, and K. Wüthrich. 1994b. The NMR structure of the pulmonary surfactant-associated polypeptide SP-C in an apolar solvent contains a valyl-rich α-helix. *Biochemistry.* 33: 6015–6023.

Knebel, D., M. Sieber, R. Reichelt, H. J. Galla, and M. Amrein. 2002. Scanning force microscopy at the air-water interface of an air bubble coated with pulmonary surfactant. *Biophys. J.* 82:474–480.

Kramer, A., A. Wintergalen, M. Sieber, H. J. Galla, M. Amrein, and R. Guckenberger. 2000. Distribution of the surfactant-associated protein C

within a lung surfactant model film investigated by near-field optical microscopy. *Biophys. J.* 78:458–465.

Krol, S., M. Ross, M. Sieber, S. Kunneke, H. J. Galla, and A. Janshoff. 2000. Formation of three-dimensional protein-lipid aggregates in monolayer films induced by surfactant protein B. *Biophys. J.* 79:904–918.

Kubitscheck, U., and R. Peters. 1998. Localization of single nuclear pore complexes by confocal laser scanning microscopy and analysis of their distribution. *Methods Cell Biol.* 53:79–86.

Lee, K. Y. C., M. M. Lipp, D. Y. Takamoto, E. Ter-Ovanesyan, J. A. Zasadzinski, and A. J. Waring. 1998. Apparatus for the continuous monitoring of surface morphology via fluorescence microscopy during monolayer transfer to substrates. *Langmuir.* 14:2567–2572.

Lee, K. Y. C., M. M. Lipp, J. A. Zasadzinski, and A. J. Waring. 1997. Understanding the nature of interactions between lipids and engineered lung surfactant proteins for better replacement therapy. *Biophys. J.* 72:WP368–WP368.

Lipp, M. M., K. Y. C. Lee, D. Y. Takamoto, J. A. Zasadzinski, and A. J. Waring. 1998. Coexistence of buckled and flat monolayers. *Phys. Rev. Lett.* 81:1650–1653.

Möhwald, H. 1990. Phospholipid and phospholipid-protein monolayers at the air/water interface. *Ann. Rev. Phys. Chem.* 41:441–476.

Nag, K., J. G. Munro, S. A. Hearn, J. Rasmusson, N. O. Petersen, and F. Possmayer. 1999. Correlated atomic force and transmission electron microscopy of nanotubular structures in pulmonary surfactant. *J. Struct. Biol.* 126:1–15.

Nag, K., J. Perez-Gil, A. Cruz, and K. M. Keough. 1996. Fluorescently labeled pulmonary surfactant protein C in spread phospholipid monolayers. *Biophys. J.* 71:246–256.

Notter, R. H., S. A. Tabak, and R. D. Mavis. 1980. Surface properties of binary mixtures of some pulmonary surfactant components. *J. Lipid Res.* 21:10–22.

Oliveira, O. N., and C. Bonardi. 1997. The surface potential of Langmuir monolayers revisited. *Langmuir.* 13:5920–5924.

Perez-Gil, J., K. Nag, S. Taneva, and K. M. Keough. 1992. Pulmonary surfactant protein SP-C causes packing rearrangements of dipalmitoylphosphatidylcholine in spread monolayers. *Biophys. J.* 63:197–204.

Possmayer, F. 1988. A proposed nomenclature for pulmonary surfactant-associated proteins. *Am. Revtl. Respir. Dis.* 138:990–989.

Post, A., A. V. Nahmen, M. Schmitt, J. Ruths, H. Riegler, M. Sieber, and H. J. Galla. 1995. Pulmonary surfactant protein C containing lipid films at the air-water interface as a model for the surface of lung alveoli. *Mol. Membr. Biol.* 12:93–99.

Qanbar, R., and F. Possmayer. 1995. On the surface activity of surfactant-associated protein C (SP-C): effects of palmitoylation and pH. *Biochim. Biophys. Acta.* 1255:251–259.

Schilling, Jr., J. W., R. T. White, and B. Cordell. 1987. Recombinant alveolar surfactant protein. USA patent 4,659,805.

Schurch, S., F. H. Green, and H. Bachofen. 1998. Formation and structure of surface films: captive bubble surfactometry. *Biochim. Biophys. Acta.* 1408:180–202.

Schurch, S., D. Schurch, T. Curstedt, and B. Robertson. 1994. Surface activity of lipid extract surfactant in relation to film area compression and collapse. *J. Appl. Physiol.* 77:974–986.

Shelly, S. A., J. U. Balis, J. E. Paciga, C. G. Espinoza, and A. V. Richman. 1982. Biochemical composition of adult human lung surfactant. *Lung.* 160:195–206.

Simons, K., and D. Toomre. 2000. Lipid rafts and signal transduction. *Nat. Rev. Mol. Cell Biol.* 1:31–39.

Skinner, F. K., Y. Rotenberg, and A. W. Neumann. 1989. Contact angle measurements from the contact diameter of sessile drops by means of a modified axisymmetric drop shape analysis. *J. Colloid Interface Sci.* 130:25–34.

von Nahmen, A., A. Post, H. J. Galla, M. Sieber. 1997a. The phase behavior of lipid monolayers containing pulmonary surfactant protein C studied by fluorescence light microscopy. *Eur. Biophys. J.* 26:359–369.

von Nahmen, A., M. Schenk, M. Sieber, M. Amrein. 1997b. The structure of a model pulmonary surfactant as revealed by scanning force microscopy. *Biophys. J.* 72:463–469.

Weaver, T. E. 1988. Pulmonary surfactant-associated proteins. *Gen. Pharmacol.* 19:361–368.

Wintergalen, A. 1999. Lungensurfactant Protein C vermittelte Vesikelfusion an der Wasser-Luft-Grenzfläche: Ausbildung von Multischichtstrukturen zur Anpassung der Oberflächenspannung. Ph.D. thesis. Westfälische Wilhelms-Universität, Muenster, Germany.

Woodle, M. C., D. Papahadjopoulos. 1989. Liposome preparation and size characterization. *Methods Enzymol.* 171:193–217.